AFOSR-TR- 78-1150

LEVEL II

AD A057064

AD No. /
DDC FILE COPY

DDC
RECEIVED
AUG 3 1978
D

Approved for public release;
distribution unlimited.

78 07 20 001

AIR FORCE OFFICE OF SCIENTIFIC RESEARCH (AFSC)
NOTICE OF TRANSMITTAL TO DDC
This technical report has been reviewed and is
approved for publication IAW AFR 190-12 (7b).
Distribution is unlimited.
A. D. BLOSE
Technical Information Officer

AIR FORCE OFFICE OF SCIENTIFIC RESEARCH (AFSC)
NOTICE OF TRANSMITTAL TO DDC
This technical report has been reviewed and is
approved for publication IAW AFR 190-12 (7b).
Distribution is unlimited.
A. D. BLOSE
Technical Information Officer

AIR FORCE OFFICE OF SCIENTIFIC RESEARCH (AFSC)
NOTICE OF TRANSMITTAL TO DDC
This technical report has been reviewed and is
approved for publication IAW AFR 190-12 (7b).
Distribution is unlimited.
A. D. BLOSE
Technical Information Officer

UNCLASSIFIED

SECURITY CLASSIFICATION OF THIS PAGE *(When Data Entered)*

(19) **REPORT DOCUMENTATION PAGE**

READ INSTRUCTIONS BEFORE COMPLETING FORM

(18) 1. REPORT NUMBER: AFOSR TR-78-1150 ✓

2. GOVT ACCESSION NO.

3. RECIPIENT'S CATALOG NUMBER

(6) 4. TITLE *(and Subtitle)*: A Model of the Human Eye-Level Blood Flow Responding to G Stress.

5. TYPE OF REPORT & PERIOD COVERED: Final Scientific rept March 1, 1977-March 1,1978

(14) 6. PERFORMING ORG. REPORT NUMBER: U D-983 ✓

(10) 7. AUTHOR(s): James J. Freeman

(15) 8. CONTRACT OR GRANT NUMBER(s): ✓ AFOSR-77-3262

9. PERFORMING ORGANIZATION NAME AND ADDRESS
University of Detroit
4001 West McNichols
Detroit, Michigan 48221

10. PROGRAM ELEMENT, PROJECT, TASK AREA & WORK UNIT NUMBERS
61102F 2312 D9

11. CONTROLLING OFFICE NAME AND ADDRESS
AFOSR (NL)
Bolling AFB, D.C. 20332

(16) (17) 12. REPORT DATE: 21 May 1978

(11) 13. NUMBER OF PAGES

14. MONITORING AGENCY NAME & ADDRESS *(if different from Controlling Office)*

(12) 37 p.

15. SECURITY CLASS. *(of this report)*: Unclassified

15a. DECLASSIFICATION/DOWNGRADING SCHEDULE

16. DISTRIBUTION STATEMENT *(of this Report)*

Approved for Public Release;
Distribution Unlimited

(9) Final scientific rept. 1 Mar 77-1 Mar 78,

17. DISTRIBUTION STATEMENT *(of the abstract entered in Block 20, if different from Report)*

18. SUPPLEMENTARY NOTES

19. KEY WORDS *(Continue on reverse side if necessary and identify by block number)*

Eye-level Blood Flow, Model, G Stress

+Gz cut z

20. ABSTRACT *(Continue on reverse side if necessary and identify by block number)*

A mathematical model of the closed loop human blood flow regulation system was derived from temporal arterial responses to +Gz stress in relaxed humans. An ensemble-average G to blood flow transfer function based on four subjects' responses to 28 +Gz stress runs was obtained on the USAFSAM human centrifuge. An analytic transfer function was fitted to the empirical function for frequencies from 5 to 200 mHz. The predictive performance

DD FORM 1 JAN 73 1473 EDITION OF 1 NOV 65 IS OBSOLETE

UNCLASSIFIED 111 300

SECURITY CLASSIFICATION OF THIS PAGE *(When Data Entered)*

20. ABSTRACT (cont'd)

of the individual subjects ensemble-averaged transfer function and the analytic transfer function was examined by comparing the actual blood flow response to the predictive responses. Within the control conditions, the analytic transfer function predicted the blood flow response with reasonable accuracy.

LEVEL II

A MODEL OF THE HUMAN EYE-LEVEL BLOOD FLOW RESPONDING TO G STRESS

James J. Freeman
University of Detroit
4001 West McNichols
Detroit, Mich. 48221

May 21, 1978

Final Scientific Report for Period 1 March 1977 - 1 March 1978

Approved for Public Release;
Distribution Unlimited

Prepared for

AIR FORCE OFFICE OF SCIENTIFIC RESEARCH
NL
Building 410
Bolling AFB, D.C. 20332

Preface

This work on eye-level blood flow responses to $+G_z$ stress is an extension of the work performed at USAFSAM in 1976 which modeled eye-level blood pressure versus $+G_z$ stress[1]. At that time excellent predictive accuracy was obtained in relating mathematically derived blood pressure responses to actual blood pressure data obtained during $+G_z$ stress on relaxed humans. At the same time the blood pressure data was being generated by placing an 18-gauge catheter in the left radial artery, a Doppler blood flowmeter was placed on the surface of the skin over the temperal artery. Therefore, data for the previous work on blood pressure responses and that for this report come from the same centrifuge studies.

Assistance in the data interpretation was gratefully received from K. K. Gillingham, M.D., Ph.D. of USAFSAM and S. A. Rositano, Ph.D. of NASA/AMES. The generation of the analytic transfer function from the ensemble-averaged transfer function was accomplished by R. C. McNee, M.S. of USAFSAM on his program entitled, "A Fortran Program to Fit a Complex-Valued Transfer Function."

Materials and Methods

Four healthy males, all members of the USAFSAM Acceleration Stress Panel, ranging in age from 24 to 26 volunteered for the studies which provided the data analyzed in this report. Doppler ultrasonic flowmeters were placed over the right and left temperal artery. The output flow velocities were recorded on magnetic tape.

The subjects were in a relaxed condition seated (13^{o} setback angle) on the centrifuge. Three different G stress profiles were taken: 1) gradual onset runs (GOR) with an acceleration rate of 0.067 G/sec.; 2) rapid onset runs (ROR) with an acceleration rate of 1 G/sec. and then maintained at a predetermined level for either 15 or 60 seconds, and 3) a simulated aerial combat maneuver (SACM) with a total period of 100 seconds and acceleration ranging from 0 to 1 G/sec. Profiles were chosen to challenge the subjects visual functioning without causing unconsciousness.

Each subject was told to be in a relaxed state and exposed to a GOR to the visual endpoint; 15 second RORs and at least one 60 second ROR; and from four to eleven SACMs. At least one 60 second ROR and one SACM elicited a visual endpoint on the subjects.

Discrete, finite Fourier Transforms of input G stress and output (eye-level blood flow) were obtained with a Hewlett Packard 5451A Fourier Analyzer. To prevent spectral aliasing and also convert the instantaneous blood flow to mean blood flow, both input and output signals were low-pass filtered with a 0.5 Hz. 48-db/octave Butterworth filter. Each G stress profile contained a 200 second record which was sampled at .78 seconds. The spectra, therefore, had a maximum frequency of 0.64 Hz with a resolution of 5 mHz. These sampling parameters were used for the resulting resolution and for compatability with the blood pressure study (1).

The filtered inputs and outputs were transformed to the frequency domain by the Fourier Analyzer and the individual transfer functions were generated by dividing the output eye-level blood flow (O(f)) by the $+G_z$ stress forcing function (I(f)). The ensemble-average of the G stress runs for each of the four individuals and the ensemble-average of all 28 G stress runs was calculated. The averaging process gave equal weight to each run. The rectangular, polar, and impulse reponse of the ensemble-averaged transfer functions of each individual and the total ensemble-averaged transfer functions are given in Appendix A. The first 25 frequency channels (5mHz per channel) are shown for the transfer functions. The first 50 channels (.078 seconds per channel) are shown for the impulse responses. Only the first 25 frequency channels were used, since 99.7% of the +G stress forcing energy was below .125 Hz (25 channels).

An analytic transfer function was then generated which most closely duplicates the frequency profile of the total ensemble-averaged transfer functions. A Fortran program was used to fit the complex-valued ensemble-averaged transfer function (2). The analytic transfer functions sought were:

1) triple pole
2) double zero - double pole
3) single zero - double pole - delay
4) single zero - triple pole - delay
5) double pole - delay - 90^{o} rotation

Parameter estimates were obtained for each analytic term by minimizing the weighted sum of the squared error for both real and imaginary terms over the first 25 frequencies. Marquardts' algorithm, combining the Taylor series expansion and negative gradient methods, was used in the computations.

Predictions of eye-level blood flow responses to GOR, ROR, and SACM G stresses, based on the actual response, the mean actual response of the individual and the response gen-

erated by the analytic transfer function, with the least standard error was obtained. Such comparisons gave visual evidence of the bidirectional aspects of the transfer functions and the range of response error involved.

Results

The mean transfer function for all 28 G stress runs is given in Appendix A. The relatively smooth, well-defined, contours of most of the empirically determined transfer functions enabled the use of simple analytical estimates of a mathematically derived function. The various equations chosen for a possible fit with the standard error are shown in Table 1. A mathematical derivation relating G stress to blood pressure and blood flow was done in order to justify the analytic functions. This derivation is shown in Appendix B.

As can be seen from Table 1 and the derivation in Appendix B, the analytic function which best fits the ensemble-averaged transfer function should and is a gain, delay, differentiator, and three poles. A comparison of this analytic transfer function and the one generated for the relationship of eye-level blood pressure versus $+G_z$ stress was also accomplished.

The analytic function with the best fit for eye-level blood pressure as a function of $+G_z$ stress was:

$$H(s) = -18.3 \frac{1 + 7.18s + 4.39s^2}{1 + 3.99s + 7.93s^2}$$

The analytic function with the best fit for eye-level blood flow as a function of $+G_z$ stress was

$$H(s) = \frac{-.936s \; e^{-2.79s}}{1 + .741s - 2.68s^2 - 29.9s^3}$$

This would mean that the relationship:

$$\frac{BF}{BP} = \frac{\text{delay - differentiator}}{\text{3 poles}}$$

would be the simplest relationship of eye-level blood flow and pressure. This relationship also is logical for pressure and

Analytical Function	Standard Error
$\frac{-.103}{(1 - 1.80s + 2.71s^2 - 15.2s^3)}$	.0477
$\frac{-.539s\ (1 - .0718s)}{1 + 3.04s + 11.8s^2}$	.0365
$\frac{-.537s\ e^{-.115s}}{1 + 3.04s + 11.7s^2}$	.0364
$\frac{-.119\ e^{j(\frac{\pi}{2} - 1.39\omega)}}{1 + 2.09(j\omega) + 6.12(j\omega)^2}$	.0347
$\frac{-.936s\ e^{-2.79s}}{1 + .741s - 2.68s^2 - 29.9s^3}$	.0295

Table 1

Analytical Functions Used as Estimates of the Transfer Function Relating $+G_z$ Stress to Eye-Level Blood Flow

flow in an artery as shown in Appendix B. The differentiator and delay would also occur since different arteries were used for the two studies. Thus, the differentiator and, especially, the delay could be due to a combination of the theoretical derivation and data collection procedure.

A mean square error analysis of the analytic transfer function (TF_{reg}) and the ensemble-averaged transfer function for each individual was also accomplished. This analysis is shown in Table 2. This analysis was done on a channel (5mHz) basis and a total square error basis. The analysis showed that individual number 3 had a drastically different transfer function frequency profile from the other three volunteers. Therefore, in the final results, the analysis of the blood flow generated by $+G_z$ stress profiles for volunteer number 3 was neglected. This analysis also showed aberrant points of volunteer number 4 in channel number 5, and its subsequent second and third harmonics. Since these frequencies had a abnormally large error, further analysis of the source of those frequencies was done. It was noted that a transient on the G stress curve was the maximum contributor to those points. Therefore, it was smoothed to compare more favorably with the other ensemble-average transfer functions.

Since the usefulness of the analytic transfer function is not in how accurately it resembles the ensemble-averaged transfer function, but in how well it predicts actual blood flow responses. We compared the actual response, the response predicted by the individual subjects' mean ensemble-averaged transfer function, and the result predicted by the analytic function. These curves are shown in Appendix C.

Data interpretation of the responses was done visually and by the HP5451A Fourier Analyzer Unit. The two main points that are easily visualized are: 1) the erratic actual response of subject number 3, and 2) the bidirectional flow characteristic of both the analytic transfer function and the ensemble-averaged transfer function.

COMPARISON OF TRANSFER FUNCTIONS

$$| TF' - TF'' |^2$$

TABLE 2

CHANNEL (5mH/ch)	$TF_{reg}, \overline{TF}_{all}$	$TF_{reg}, \overline{TF}_1$	$TF_{reg}, \overline{TF}_2$	$TF_{reg}, \overline{TF}_3$	$TF_{reg}, \overline{TF}_4$	$\overline{TF}_1 \quad \overline{TF}_4$	$\overline{TF}_2 \quad \overline{TF}_4$	$\overline{TF}_1 \quad \overline{TF}_2$
1	.002	.07	0	25	.03	.02	.83	1.08
2	.001	.16	.65	536	.27	.18	.48	.10
3	.001	.15	.47	626	.14	.05	1.22	1.65
4	.003	.07	.97	436	.31	.17	1.91	.95
5	.002	.51	.82	114	1.03	.10	.83	.42
6	.001	.58	.71	1730	.15	.16	.19	0
7	.003	.45	.62	353	.62	.03	.63	.40
8	.002	.21	.17	1153	.71	.22	0	.26
9	.001	.82	.76	26	.74	.16	1.41	.66
10	.003	.36	1.4	209	.84	.16	.21	.32
11	.003	.17	1.4	203	.95	.32	.06	.12
12	.005	.53	.57	538	.56	.15	.60	1.13
13	.002	.49	2.2	29	.44	.21	.09	.03
14	0	.22	.33	71	.38	.13	1.32	2.25
15	.002	.39	2.69	200	.02	.57	.27	.39
16	.002	.29	.25	108	.50	1.37	.44	.35
17	.003	.43	0	8	.38	.23	.52	.63
18	.007	.55	.02	981	.02	.78	0	.77
19	.001	.19	.02	13	.26	.80	.21	.24
20	.002	.26	0	1	.39	1.08	.34	.34
21	0	.24	0	40	1.58	2.12	1.68	.29
22	.001	.32	0	3	.84	2.17	.79	.35
23	.002	.007	.01	302	.71	1.12	.62	.02
24	.001	.31	0	47	1.08	1.60	1.09	.34
25	0	0	0	70	.99	.97	.97	0
Total	.05	7.8	13.3	7910	13.0	14.8	16.1	13.1

Due to the erratic behavior of the flow responses of subject number 3, his actual strip chart recording data was again analyzed visually. It was noted that in most of his runs, blood flow and blood pressure increased before the decrease in $+G_z$ stress. This could be explained if the subject did not remain in the relaxed state for the entire run. Another possible cause of this erratic flow could be the state of the art of the Doppler flowmeter at that time (1974). The transducer and signal analysis of the system had yet to be optimized. These erratic responses were not noted in the previous blood pressure study, since they did not affect the blood pressure as drastically. This could be due to increased sensitivity of the blood flow data. That is, percentage-wise, the blood flow data changed more than the blood pressure with similar changes in $+G_z$ stress.

The bidirectional flow aspect of the predicted responses were changed to unidirectional, while allowing for some negative flow, by inserting a weighted amplifier on the output of the HP5451A analyzer. This weighted amplifier is shown in Figure 1.

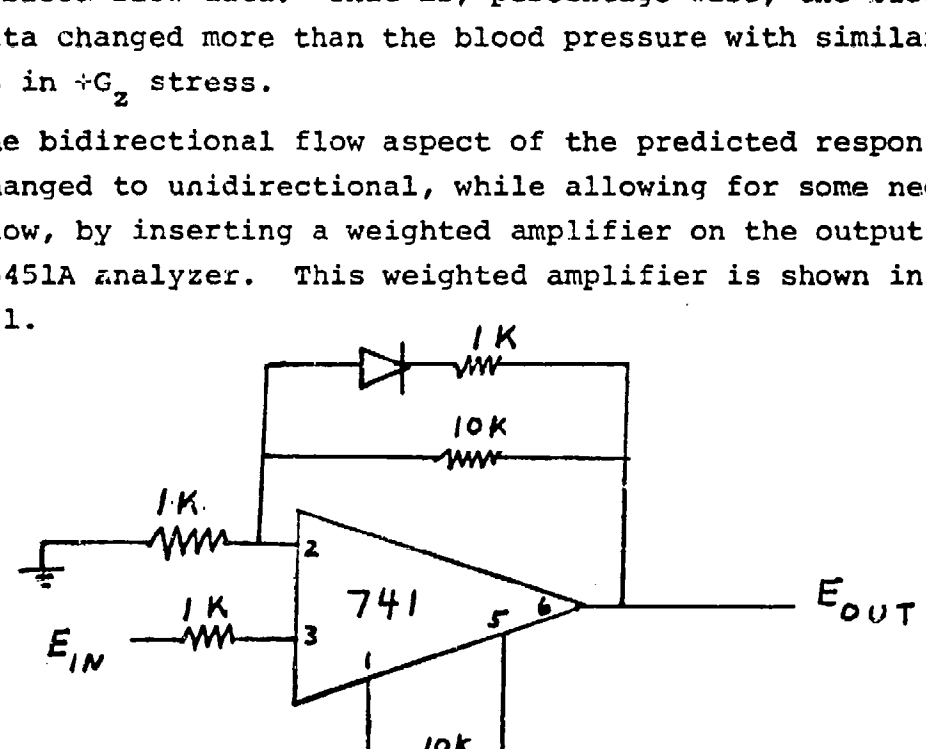

Figure 1
Circuit for Changing Bidirectional Flow
to Weighted Unidirectional Flow

The dashed line on $+G_z$ stress runs 4506, 10936, 10530, 13100, 2300, 3906, and 2730 in Appendix C are generated with the weighted amplifier to simulate unidirectional flow.

The time error analysis was done on the HP5451A Fourier Analyzer. The analysis compared the time differences between the actual response and the predicted response from the analytic transfer function responding to the 28 $+G_z$ stress profiles. The maximum and minimum points on the responses, along with the initial point of zero flow, were compared.

The results of this analysis are:

Time Differentials for Maximum and Minimum Points

Mean = 1.5 seconds

Maximum = 4.5 seconds

Time Differentials for the Onset of Zero Flow

Mean: 1.2 seconds

Maximum: 5.0 seconds

The mean time differences between the actual response and the response generated by the analytic transfer function are well within useful and anticipated errors.

Discussion

Linear systems analysis techniques were used to model nonlinear systems. This limitation was deemed minimal, since the ensemble-averaged transfer function for the 28 G stress profiles correlated well with the delay-differentiator three pole analytic transfer function. The correlation was comparable to that of the blood pressure -G stress analytic transfer function (1).

The blood flow data was generated with a Doppler ultrasonic system which cannot yield accurate quantitative data due to the various incident phase angles encountered. The results, however, are modeled for percent magnitude changes, and, therefore, numerical values are not needed.

The data presented in this report has been theoretically compared to the previous work on blood pressure response to G stress profiles. There is no other work which could be used for comparison that includes blood flow data as a function of G stress.

The time analysis of the data shows a mean time delay between the actual response and the analytically generated response of 1.5 seconds for maxima and minima and 1.2 seconds for the onset of zero flow. It has been shown that gray out occurs approximately 4 to 10 seconds after the onset of zero flow (6). Thus, the mean error is well within the limits for predicting gray out. The maximum time delay of 5 seconds, between actual and predicted onset of zero flow, is marginal. Thus, prediction capability may be impaired at the upper limits of error.

Since the system models eye-level blood flow of relaxed humans, it can only be a part of a real world model relating G stress to eye-level blood flow. A realistic model must incorporate straining maneuvers and the use of anti-G suits on the cardiovascular system dynamics. Since these phenomena are highly nonlinear, these effects should be modeled separately and then added to the basic blood flow control model. This would give a complete model of the physiological effects of G stress on humans. This data then could be used effectively to predict pilot performance during various aerial combat maneuvers.

Conclusion

Data describing the eye-level blood flow response to G stress in relaxed humans has been presented as an empirical G to blood flow transfer function and as a mathematically well-defined analytic function. The transfer functions cover the frequency spectrum from 5 to 200 mHZ or 99.7% of the forcing energy. The transfer functions exhibit adequate predictive ability within the forcing function parameters (1.0 → 4.5G; 0 → 200 seconds). The transfer functions were modified by

an operational amplifier circuit to enhance the unidirectional flow with weighted reverse flow. The delay-differentiator three pole function most closely fits the empirical transfer function and predicts eye-level blood flow with usable accuracy.

Bibliography

1. Gillingham, K. K., Freeman, J. J., McNee, R. C., "Transfer Functions for Eye-Level Blood Pressure during $+G_z$ Stress," Aviation, Space, and Environmental Medicine, 11/1977, pp. 1026-1034.

2. McNee, R. C., "A Fortran Program to Fit a Complex-Valued Transfer Function," Internal Report USAF School of Aerospace Medicine, Aerospace Medical Division.

3. Middleman, S., "Transport Phenomena in the Cardiovascular System," Chapter 5, John Wiley & Sons, 1972.

4. Fung, Y. C., Perrone, N., Anliher, M., "Biomechanics," Chapter 5, Prentice-Hall, 1972.

5. Attinger, E. O., "Pulsative Blood Flow," Chapter 2, University Microfilms, 1970.

6. Personal Communication with S. Rositano of NASA/AMES.

APPENDIX A

The frequency characteristics of the various transfer functions used are given in rectangular and polar coordinates. The frequency coordinates are given in the left column. The frequency value is equal to the column number multiplied by .005 HZ.

The "SF" code is translated below

SF A B C

A — Magnitude scale factor (10^A)

B — 4 = Rectangular coordinates

5 = Polar coordinates

0 = Time coordinates

C — Sampling period code (22 = 200 seconds)

We0 0 25

SF	-3	4	22					
(| 0)	0	0	193	-234	-167	-461	-97	-461
(| 4)	-257	-227	-480	-739	-802	-419	-689	-455
(| 8)	-594	-75	-1110	147	-796	-108	-583	-16
(| 12)	-881	-122	-723	452	-205	555	-681	327
(| 16)	-451	378	-453	651	-424	769	91	482
(| 20)	379	442	332	429	517	282	99	85
(| 24)	428	393	0	0				

TF0

We0 0 25

SF	-3	5	22					
(| 0)	0	0	303	-5041	490	-10984	471	-10186
(| 4)	343	-13857	881	-12299	904	-15241	825	-14660
(| 8)	599	-17281	1120	17240	804	-17235	583	-17844
(| 12)	889	-17212	853	14795	592	11025	756	15427
(| 16)	589	13994	793	12477	878	11883	491	7942
(| 20)	583	4943	542	5234	589	2869	131	4080
(| 24)	582	4262	0	0				

We0 0 50

SF	-2	0	22						
(	0)	-1497	-1827	-2038	-2000	-1790	-1205	-453	428
(	8)	1272	1944	2354	2420	2290	1822	1253	672
(	16)	284	6	-133	-23	180	430	540	657
(	24)	611	493	304	95	-85	-233	-211	-223
(	32)	-170	-108	49	111	92	116	105	85
(	40)	-46	-80	-160	-193	-216	-197	-138	-69
(	48)	123	220	322					

The Rectangular, Polar, and Impulse Response of the Averaged Transfer Function for Subject Number One

```
W 0 0 25
SF      -3       4      22
(       0)       0       0    -739     230    -439    -626    -663     692
(       4)    -526     711    -600    -800    -857    -357    -470     142
(       8)    -870    -501    -945     942   -1345    -257    -926     -58
(      12)   -1444     780    -676     274   -1695     361    -451    -257
(      16)       0       0       0       0       0       0       0       0
(      20)       0       0       0       0       0       0       0       0
(      24)       0       0       0       0

TF0

W00 0 25
SF      -3       5      22
(       0)       0       0     774   16267     764  -12502     959   13374
(       4)     885   12645    1000  -12688     928  -15738     491   16305
(       8)    1004  -15007    1334   13504    1369  -16918     928  -17647
(      12)    1642   15158     729   15787    1733   16794     519  -15030
(      16)       0       0       0       0       0       0       0       0
(      20)       0       0       0       0       0       0       0       0
(      24)       0       0       0       0

TR0

F00

W00 0 50
SF      -2       0      22
(       0)   -2528   -2503   -2368   -2066   -1699   -1222    -714    -219
(       8)     245     619     932    1059    1169    1104     973     751
(      16)     492     223     -62    -276    -473    -570    -649    -629
(      24)    -571    -476    -355    -245    -109     -36      51      69
(      32)      89      63      33      -3     -61     -75    -107     -83
(      40)     -88     -35      14      74     135     182     253     272
(      48)     320     320     345
```

The Rectangular, Polar, and Impulse Response of the Averaged Transfer Function for Subject Number Two

```
W@0 0 25
SF      -3       4      22
(        0)   -159       0     -77     727    -452     648    -393     530
(        4)     19     336   -1314     -85    -583     124     905     575
(        8)   -113    -116    -297    -351    -100     439    -467     567
(       12)   -171      22     -96     249     202    -398    -213    -252
(       16)    -89      10    -623     771    -111     -18      15      14
(       20)     11     197      30     -38    -508     211    -152    -154
(       24)     68    -202     238    -114

TP0

W@0 0 25
SF      -3       5      22
(        0)    159       0     732    9603     791   12487     660   12651
(        4)    337    8680    1317  -17631     596   16785    1072    3247
(        8)    162  -13427     459  -13026     451   10277     735   12940
(       12)    173   17249     267   11089     446   -6306     330  -13025
(       16)     89   17351     992   12891     112  -17085      21    4597
(       20)    199    8703      48   -5195     550   15732     216  -13454
(       24)    213   -7150     264   -2550

TR0

F@0

W@0 0 50
SF      -2       0      22
(        0)   -906    -942    -958    -876    -849    -709    -605    -485
(        8)   -382    -327    -304    -340    -301    -382    -439    -486
(       16)   -438    -398    -372    -253    -155     -41     -41      11
(       24)    -31     -69    -115    -183    -239    -301    -246    -262
(       32)   -228    -185     -34      81     157     304     408     486
(       40)    415     348     140     -93    -365    -638    -858   -1025
(       48)  -1004    -984    -871
```

The Rectangular, Polar, and Impulse Response of the **Averaged** Transfer Function for Subject Number Three

```
W00 0 25
SF      -3       4      22
(       0)       0       0      58    -206     245    -550    -286    -347
(       4)    -122    -609    -559   -1036    -424    -305    -716    -608
(       8)    -854    -467   -1029    -242   -1111     127   -1148      20
(      12)    -882     255    -788      -2    -553     488       0       0
(      16)     108    -649    -676     234       0       0    -356    -290
(      20)    -577      43   -1103     677    -838    -297   -1000   -1000
(      24)    -808     657    -985      -5

TP0

W00 0 25
SF      -3       5      22
(       0)       0       0     213   -7426     602   -6605     450  -12953
(       4)     621  -10126    1177  -11836     522  -14429     939  -13966
(       8)     973  -15136    1057  -16677    1118   17343    1148   17896
(      12)     918   16381     788  -17992     738   13851       0       0
(      16)     658   -8064     716   16083       0       0     459  -14088
(      20)     579   17565    1294   14842     858  -16050    1414  -13500
(      24)    1041   14085     985  -17975

TR0

F00

W00 0 50
SF      -2       0      22
(       0)   -2907   -2535   -1828    -820      75     931    1416    1593
(       8)    1462    1177     928     765     959    1192    1547    1837
(      16)    2047    1925    1484     950     307    -205    -673    -770
(      24)    -718    -489    -230     -23      85      37      60     -75
(      32)    -108     -89     121     288     367     449     395     264
(      40)     -71    -251    -437    -452    -359    -181      35     170
(      48)     336     258     141
```

The Rectangular, Polar, and Impulse Response of the Averaged Transfer Function for Subject Number Four

```
W00 0 25
SF      -4       4       0
(        0)      0       0     200    -381       0    -945    -382    -729
(        4)   -486    -587    -879   -1378   -1278    -560   -1255    -936
(        8)  -1329    -327   -2119     138   -2042      10   -1754     173
(       12)  -1721     314   -1349     711    -747    1076    -998     997
(       16)   -286     422    -702    1184    -998     997     173     528
(       20)    405     560     -35     707     199     198     199     997
(       24)     98     198      98      97

TF0

W00 0 25
SF      -4       5       0
(        0)      0       0     430   -6231     945   -9000     823  -11764
(        4)    761  -12961    1634  -12252    1395  -15634    1566  -14329
(        8)   1369  -16620    2124   17626    2042   17969    1762   17434
(       12)   1749   16961    1525   15218    1310   12474    1411   13499
(       16)    510   12402    1377   12064    1411   13499     557    7191
(       20)    692    5419     708    9279     281    4500    1017    7876
(       24)    221    6391     138    4500

W 0 0 50
W 0 0 50
SF      -3       0       0
(        0)  -3433   -3931   -4095   -3775   -3126   -1919    -503    1013
(        8)   2382    3429    4062    4183    4032    3435    2707    1947
(       16)   1407     937     557     432     377     373     214     167
(       24)     35     -69    -158    -196    -171    -146      38      86
(       32)    138     143     256     251     171     201     228     265
(       40)    136     123      15     -79    -197    -263    -262    -227
(       48)     10     155     332
```

The Rectangular, Polar, and Impulse Response of the Ensemble Averaged Transfer Function of the Four Subjects

```
W00 0 25
SF      -4      4      29
(        0)    -51       0    -150    -550    -300    -800    -550   -1000
(        4)   -800   -1050   -1120   -1020   -1420    -880   -1650    -600
(        8)  -1750    -350   -1750     100   -1600     399   -1400     599
(       12)  -1150     749    -950     849    -720     899    -550     899
(       16)   -400     879    -250     839    -150     779     -51     739
(       20)     21     659     101     599     120     549     160     499
(       24)    200     449       0       0

W 0 0 25
W 0 0 25
SF      -4      5      29
(        0)     51       0     570  -10524     854  -11056    1141  -11881
(        4)   1320  -12730    1515  -13768    1670  -14822    1755  -16002
(        8)   1784  -16869    1752   17672    1649   16595    1523   15679
(       12)   1373   14687    1275   13817    1152   12866    1055   12142
(       16)    967   11445     876   10657     794   10087     742    9387
(       20)    661    8825     608    8052     563    7770     525    7226
(       24)    493    6605       0       0

W00 0 50
W00 0 50
SF      -3      0      29
(        0)  -3228   -3838   -4142   -4024   -3499   -2510   -1240     159
(        8)   1473    2562    3302    3629    3623    3302    2832    2308
(       16)   1876    1518    1251    1094     979     857     656     467
(       24)    249      54    -109    -184    -182    -139     -38      26
(       32)     68      57      51      -3     -65     -73     -34      36
(       40)     76     157     196     205     155      99      41     -15
(       48)    -14     -10      29
```

The Rectangular, Polar, and Impulse Response
of the Mathematically Derived Transfer Function

APPENDIX B

Theory Guiding Pressure-Flow Relationship:

The steady state flow is described by Poiseuille Law. In the transient case, it is essential to attempt to formulate a precise set of equations. The nonlinearites have to be considered. Such nonlinearites arise from the tapering of arteries, elastic wall of blood vessels which expand due to pressure, etc. (3). Considering these, the equations for pressure flow based on Navier-Stoke and the continuity equations are: (4)

$$v \frac{\partial S}{\partial t} + S \frac{\partial v}{\partial t} + \frac{\partial S}{\partial t} + \psi = 0 \qquad (1)$$

$$\frac{\partial v}{\partial t} + v \frac{\partial v}{\partial Z} = - \frac{1}{\rho} \frac{\partial P}{\partial Z} + f \qquad (2)$$

where

S = area which depends on t, p, Z

p = pressure

t = time

Z = axial direction

v = velocity

ψ = term for seepage

f = gravity or centrifugal and friction forces

It has been shown (3) that with friction, etc., the equations can be written as

$$- \frac{\partial}{\partial Z} \left(S v^2 + \frac{PS}{\rho} \right) - \frac{TwD}{\rho} + \frac{P}{\rho} \frac{\partial S}{\partial Z} = \frac{\partial}{\partial t} (Sv) + \rho S g \qquad (3)$$

where

$$S = {}^{S_o}/_{1 - P \frac{D_o}{h_o E}}$$

f = friction

g = gravity

D_o and h_o are diameter and wall thickness at zero pressure conditions.

The continuity equation is

$$\frac{\partial S}{\partial t} + \frac{\partial}{\partial Z} (vS) = 0 \tag{4}$$

If flow = θ = vA, then it can be shown by algebraic manipulations that the Navier-Stoke and continuity equations take the form:

$$- \frac{\partial}{\partial Z} \left\{\frac{\theta^2(1-Pk)}{A_o}\right\} - \frac{\partial}{\partial Z} \left\{\frac{A_o P}{\rho(1-Pk)}\right\} - \frac{8\mu k(\partial)\theta}{\rho A_o} \{1-Pk\}$$

$$= \frac{A_o P}{\rho} \frac{\partial}{\partial Z} \left(\frac{1}{1-Pk}\right) = \frac{\partial \theta}{\partial t} + \frac{A_o g(t)}{1-Pk} \tag{5}$$

and

$$\frac{\partial}{\partial t} \left(\frac{1}{1-Pk}\right) + \frac{1}{A_o} \frac{\partial \theta}{\partial Z} = 0 \tag{6}$$

These equations are the general form for Navier-Stoke and continuity relationships. A solution of these nonlinear partial differential equations must be done by approximation techniques.(5)

It should be noted that pressure and flow are dependent not only on g, but on other factors. An equation, therefore, which attempts to relate p(t) and g(t) or θ(t) and g(t) directly are not real system equations. The system equations are nonlinear and given by the previously nonlinear equations.

Algebraic manipulations of the Navier-Stoke and continuity equations yields the following differential equations:

$$\frac{\partial}{\partial Z} \left\{\frac{\partial^2 P}{\partial t^2}\right\} = L_1 \frac{\partial^3 \theta}{\partial t^3} + R_1 \frac{\partial^2 \theta}{\partial t^2} + S \frac{\partial^2 g}{\partial t^2} \tag{7}$$

$$\frac{\partial^2 P}{\partial t^2} = \phi_1 Z \left\{L_1 \frac{\partial^3 \theta}{\partial t^3} + - - - S \frac{\partial^2 g}{\partial t^2}\right\}$$

$$\frac{\partial P}{\partial t} = \phi_2 Z \left\{L_1 \frac{\partial^2 \theta}{\partial t^2} + - - - S \frac{\partial g}{\partial t}\right\}$$

$$P = \phi_3 Z \left\{L_1 \frac{\partial \theta}{\partial t} + - - - S\, g(t)\right\}$$

The form of equation which relates these differential equations is:

$$\lambda_1 \frac{\partial^2 P}{\partial t^2} + \lambda_2 \frac{\partial P}{\partial t} + \lambda_3 P = \{\phi_1 Z \frac{\partial^3 \theta}{\partial t^3} + \phi_2 Z \frac{\partial^2 \theta}{\partial t^2} + \phi_3 Z \frac{\partial \theta}{\partial t} + \phi_4 Z\theta \} + \{\partial_1 Z \frac{\partial^2 g}{\partial t^2} + \partial_2 Z \frac{\partial g}{\partial t} + \partial_3 Z g\} \quad (8)$$

where λ, ϕ, γ are constants.

The above equation yields the general form of the blood pressure, blood flow, and gravitational force relationships. Note that pressure and flow are third order systems, while gravitational force is second order. This shows that the transfer functions may be of the form

$$\frac{Ke^{-as}}{1 + as + bs^2 + cs^3}$$

APPENDIX C

The eye-level blood flow responses are given for $+G_z$ stress profiles for subjects 1,2,3 and 4. The four curves are arranged in the following order.

FIRST	-	$+G_z$ stress
SECOND	-	Actual eye-level blood flow response to the stress
THIRD	-	Response generated by the individuals' ensemble-averaged transfer function to the $+G_z$ stress
FOURTH	-	Response generated by the analytic transfer function to the $+G_z$ stress

The dashed lines on the responses due to the ensemble-averaged transfer functions are due to the addition of the operational amplifier which limits reverse flow.

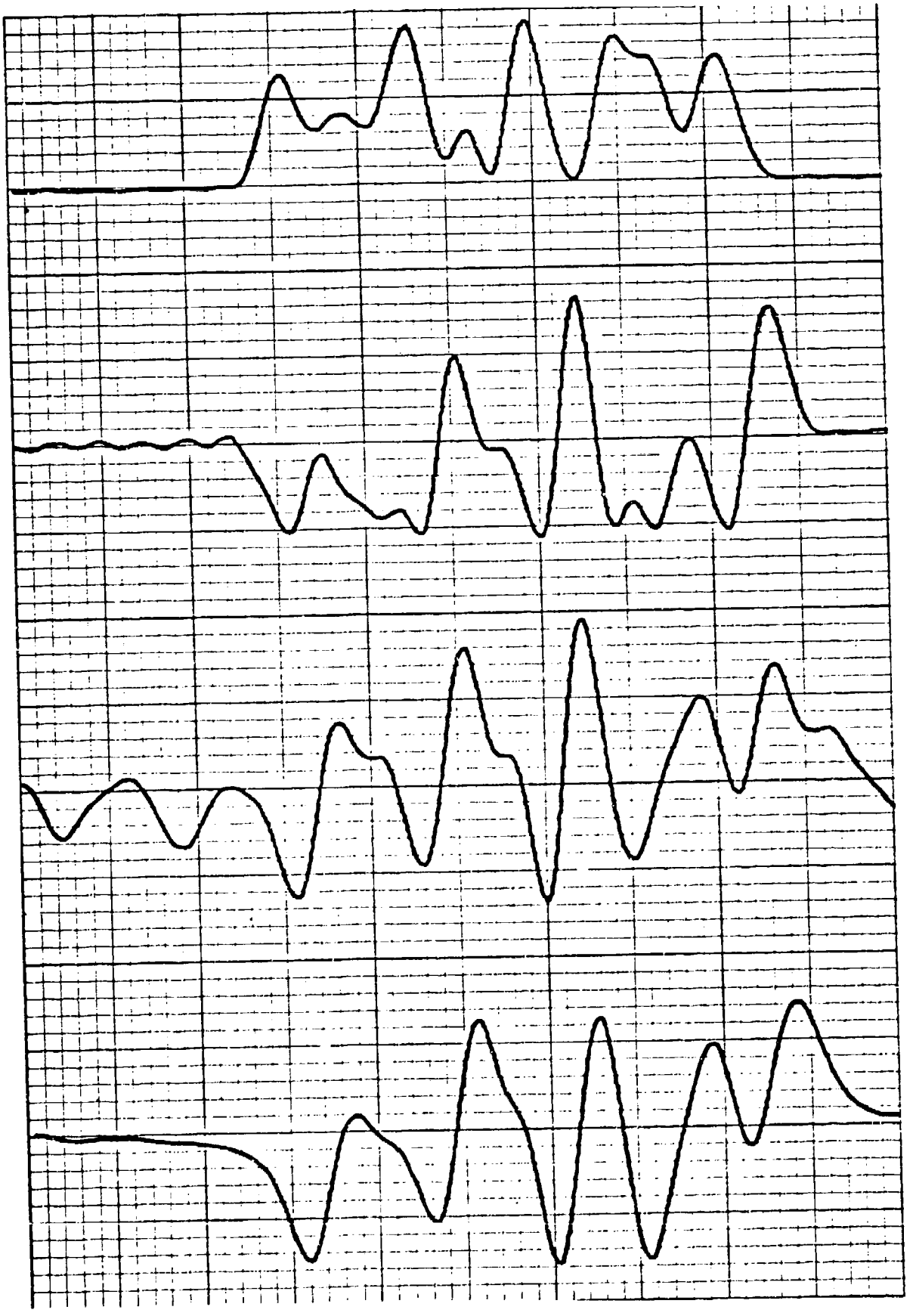

ACM - Subject Number One - Code 5930

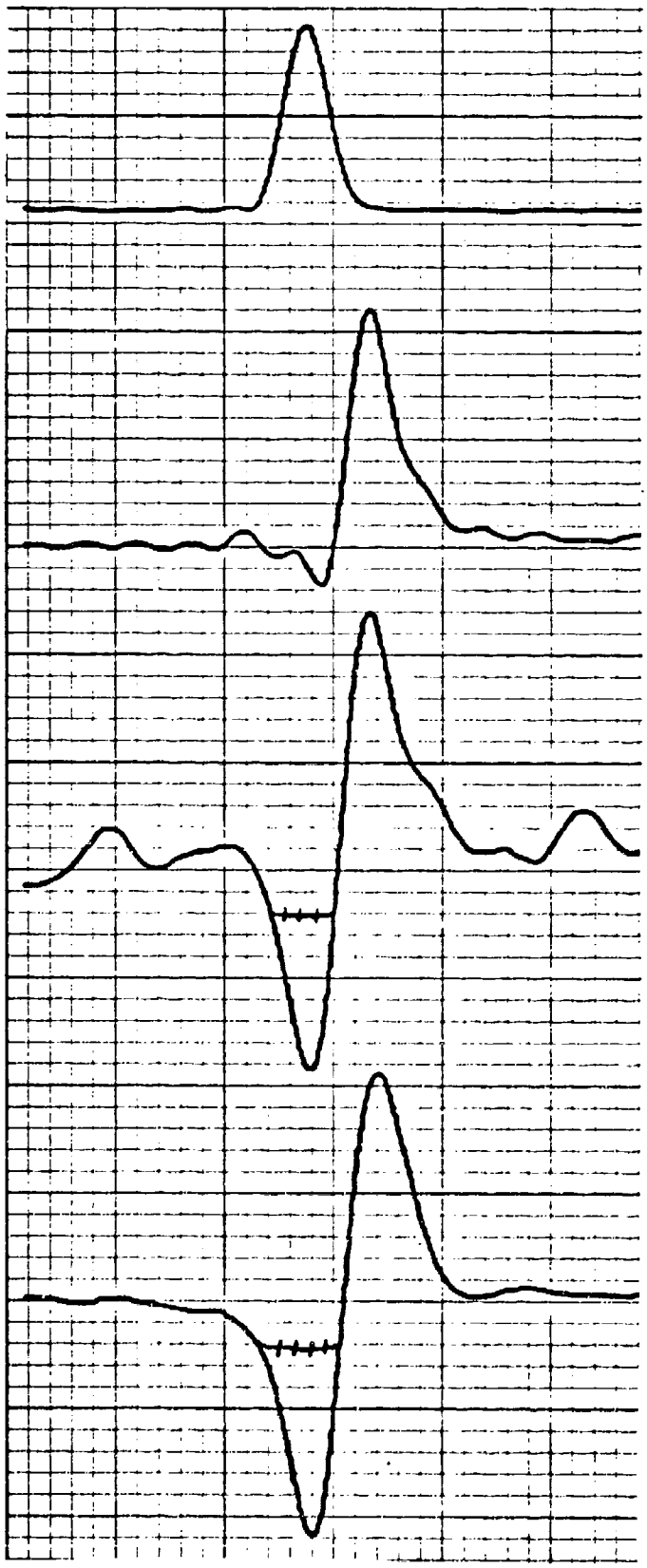

Rapid Onset Run - Subject Number One - Code 4500

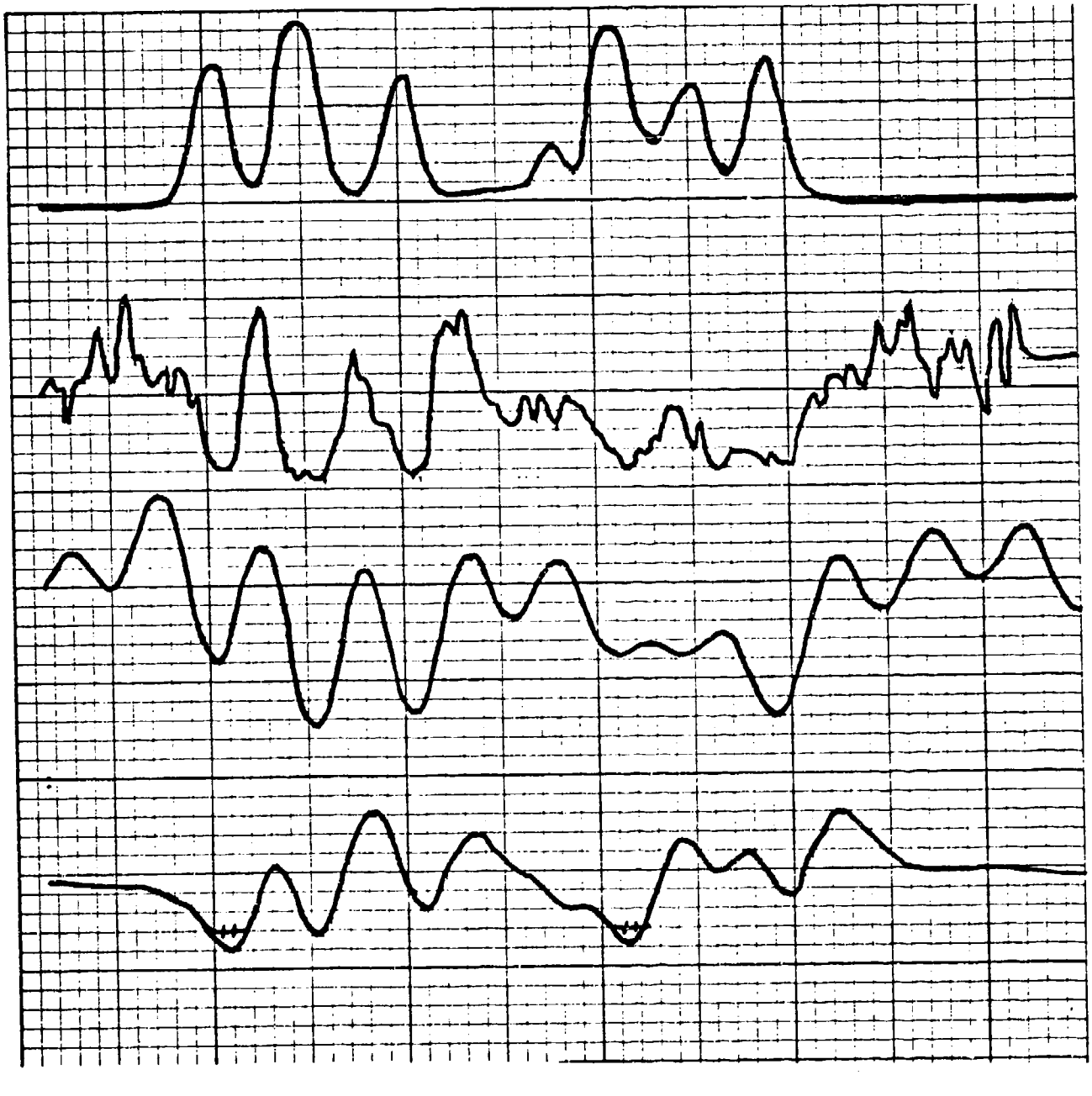

ACM - Subject Number 2 - Code 10930

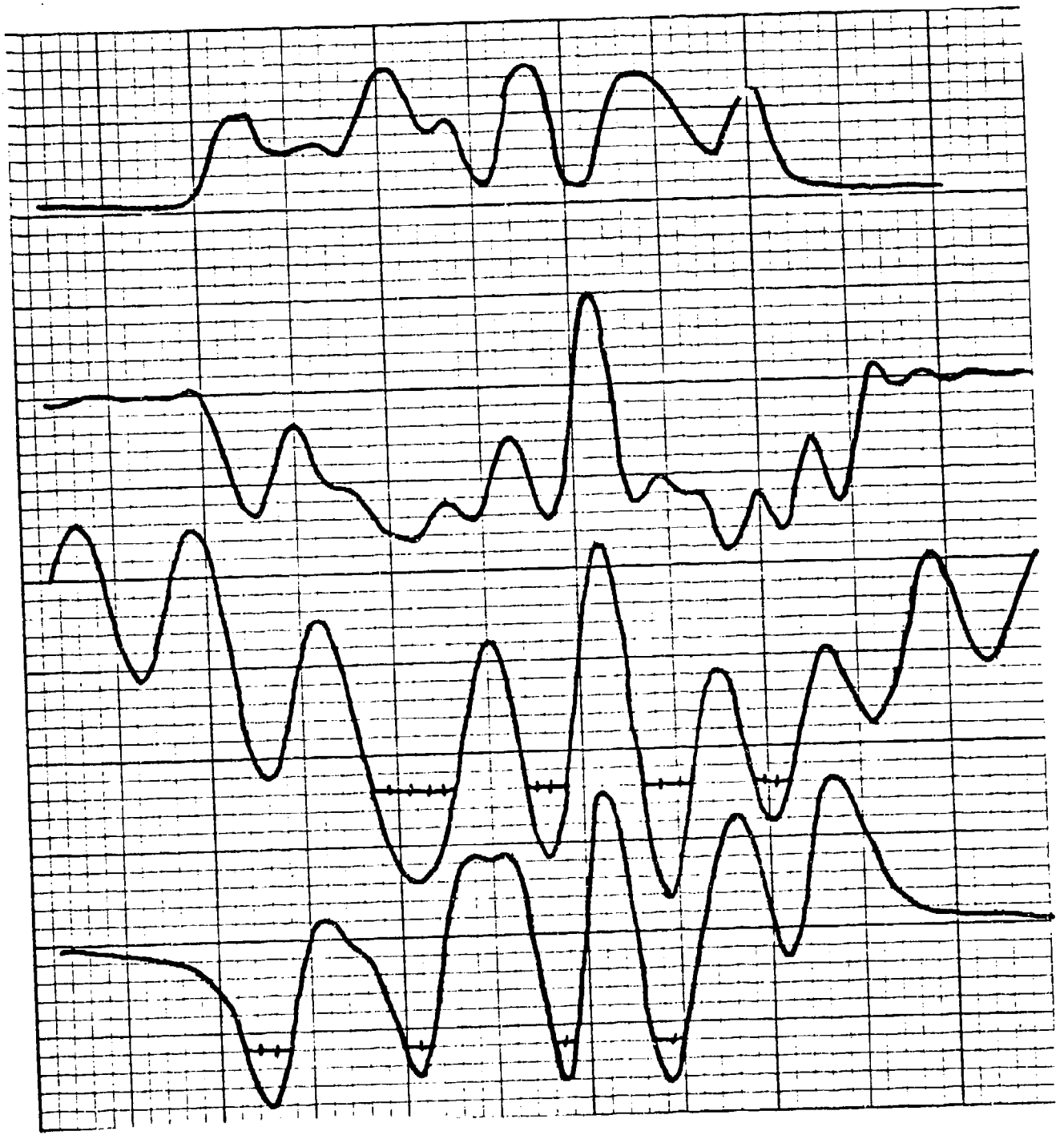

ACM - Subject Number 2 - Code 10530

ROR - Subject Number 3 - Code 12730

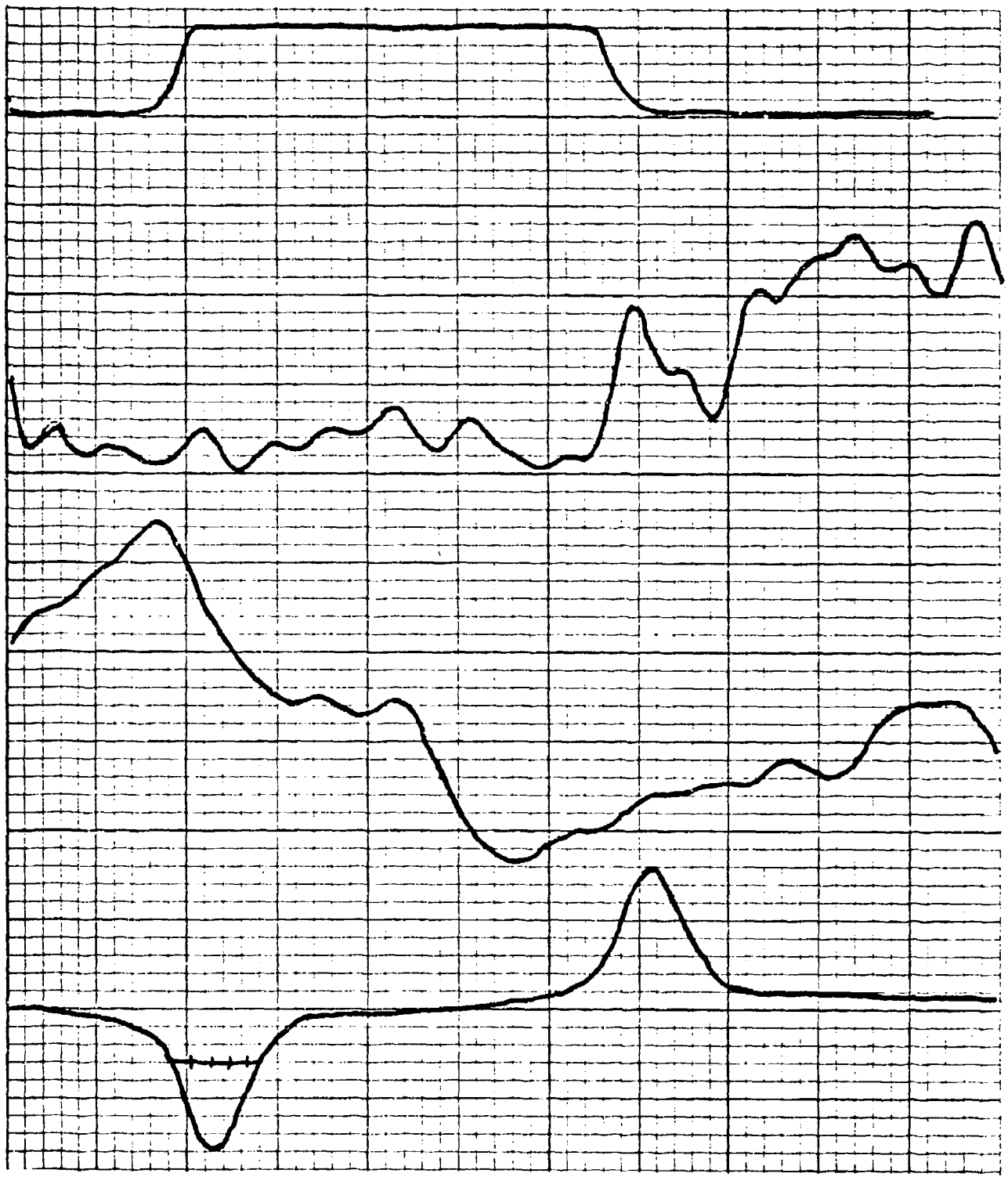

ROR - Subject Number 3 - Code 13100

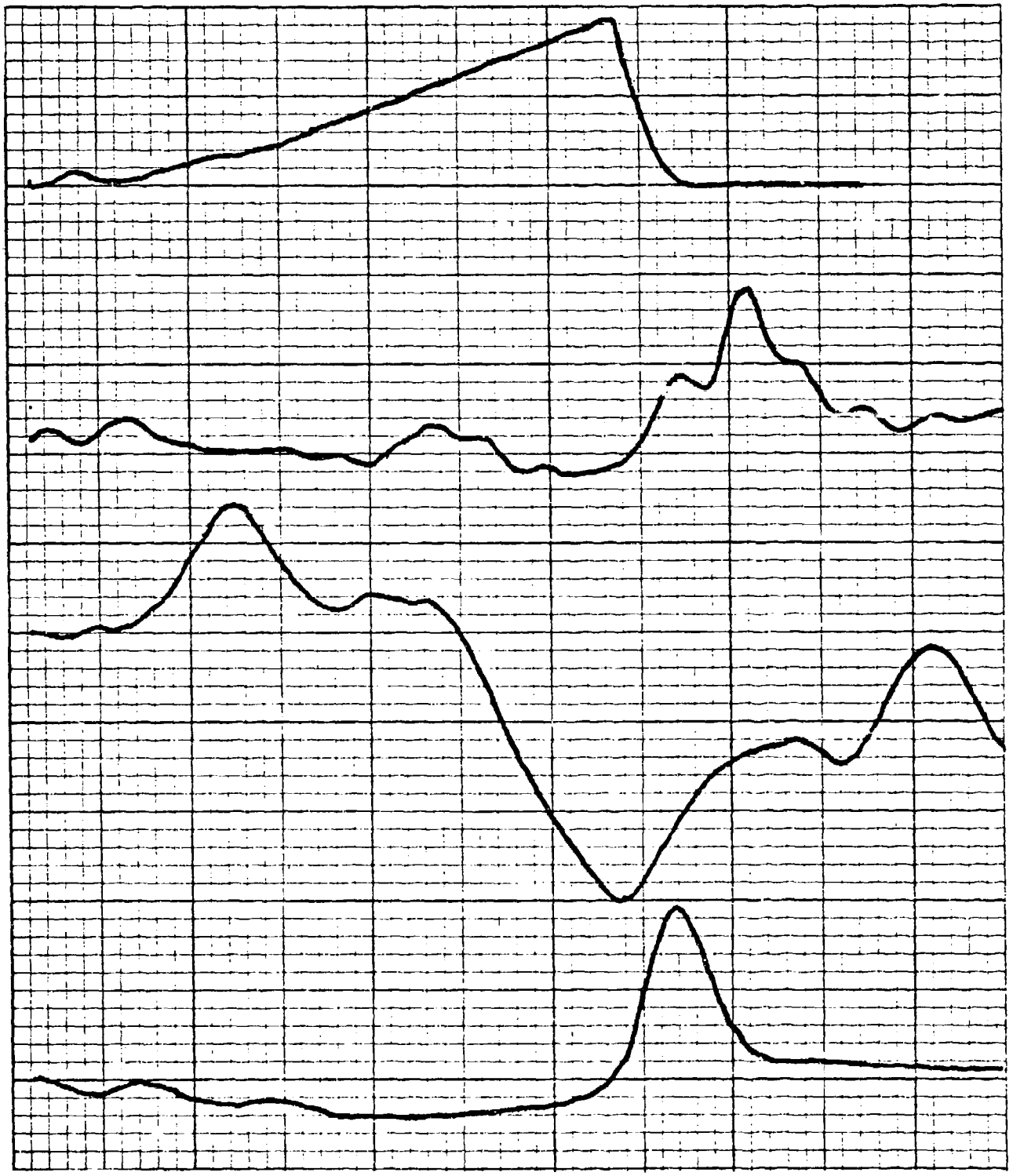

GOR - Subject Number 3 - Code 12530

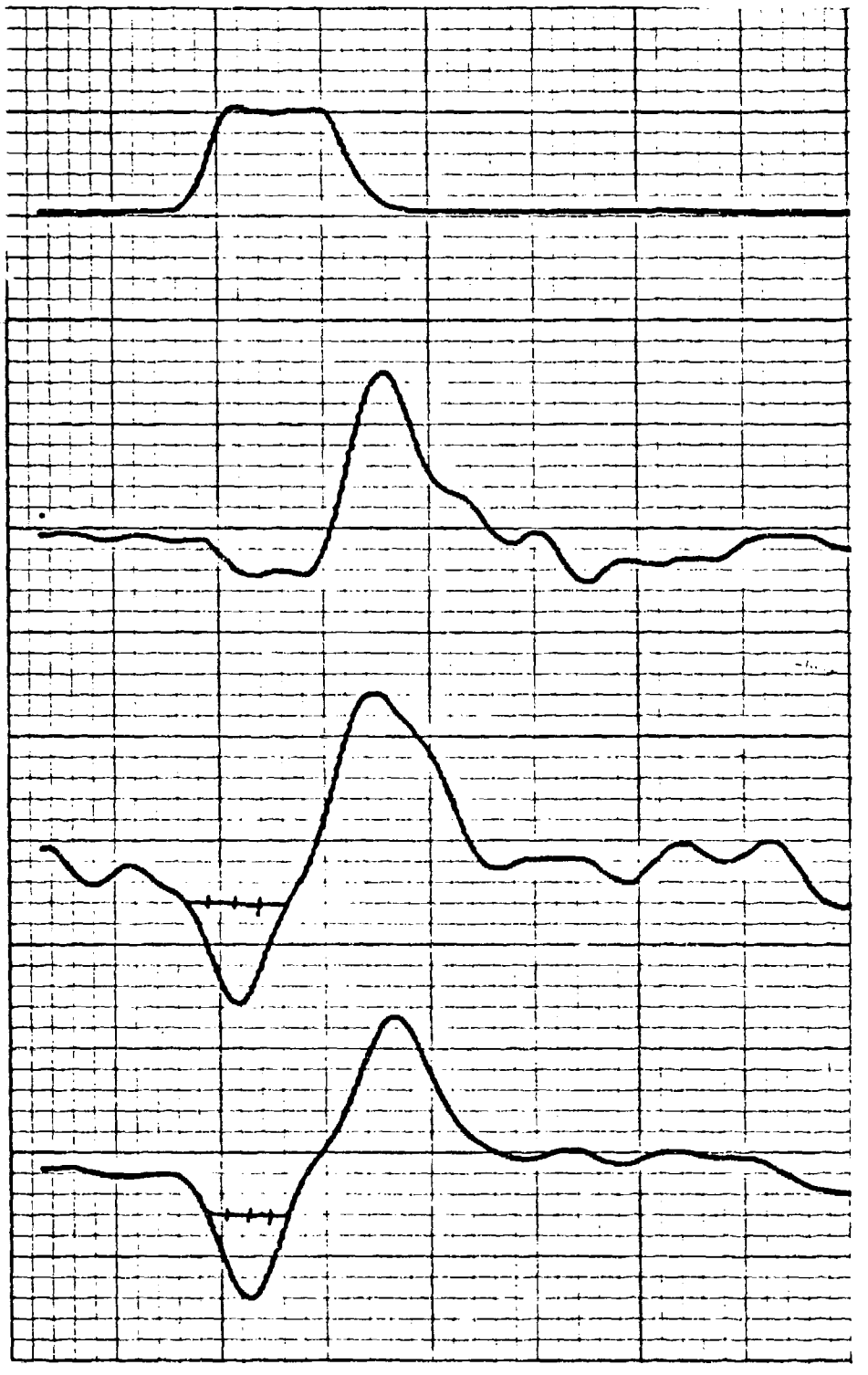

ROR - Subject Number Four - Code 2300

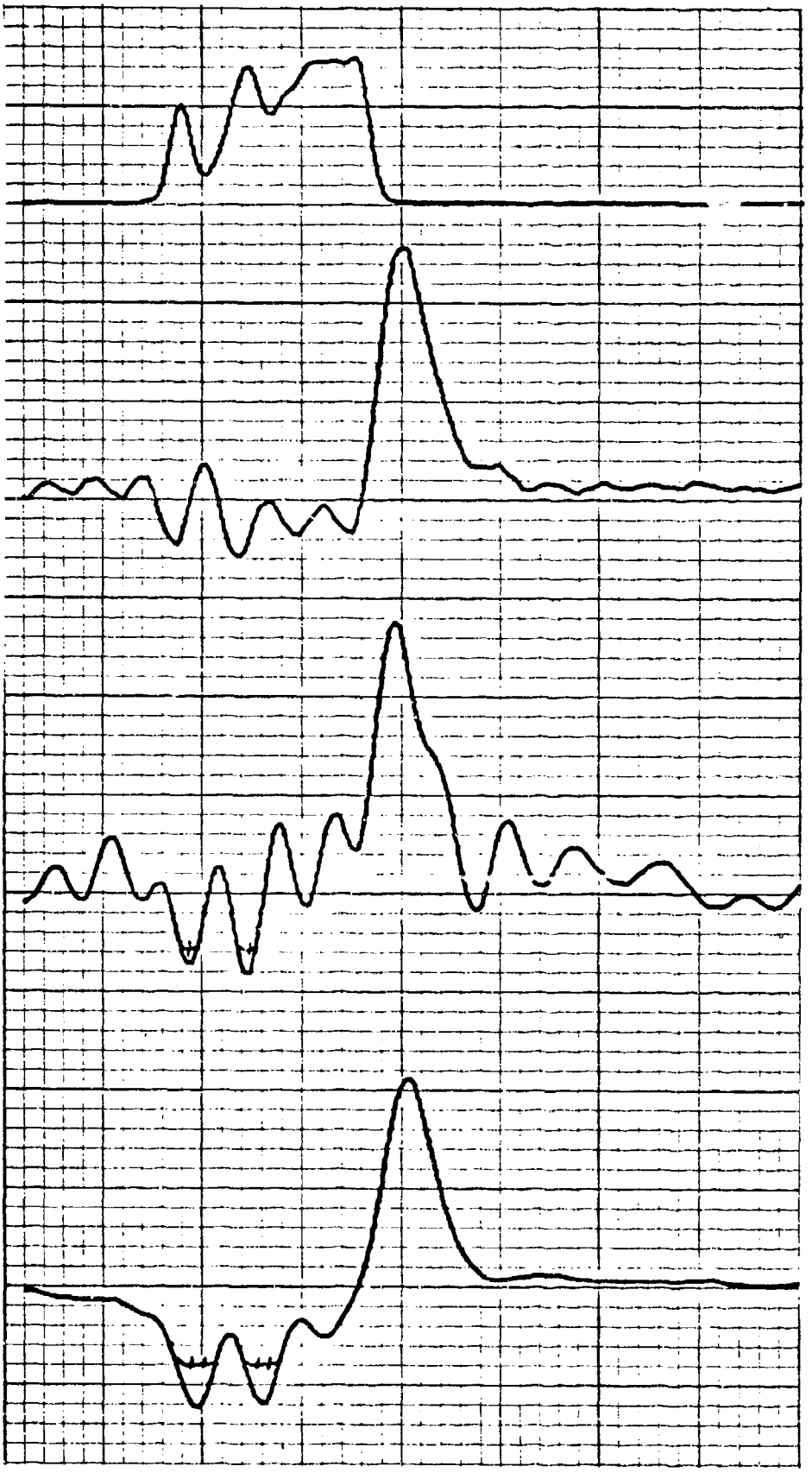

Aborted ACM - Subject Number Four - Code 3900

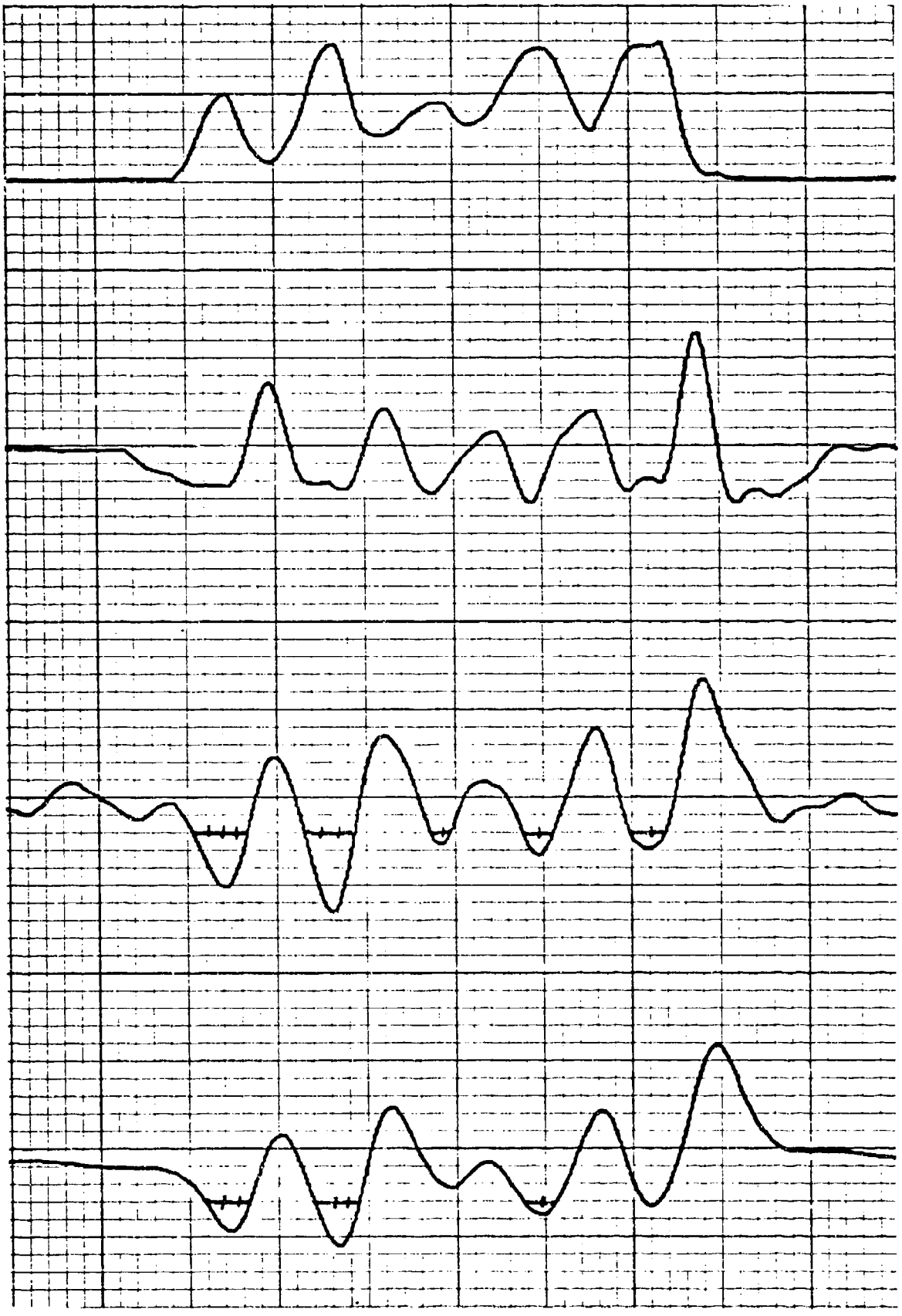

ACM - Subject Number Four - Code 2730